Eur. Phys. J. A (2020) 56:199
https://doi.org/10.1140/epja/s10050-020-00212-x

THE EUROPEAN PHYSICAL JOURNAL A

Regular Article - Experimental Physics

Indirect measurement of the ^{3}He(n,p)^{3}H reaction cross section at Big Bang energies

R. G. Pizzone[1,a], C. Spampinato[1,2,3], R. Spartá[1,2], M. Couder[4], W. Tan[4], V. Burjan[5], G. D'Agata[5], G. L. Guardo[1], M. La Cognata[1], L. Lamia[1,2,3], J. Mrazek[5], S. Palmerini[6,7], S. Typel[8,9], A. Tumino[1,10], M. Wiescher[4], S. Anguilar[4], D. Bardayan[4], D. Blankstein[4], L. Boccioli[4,6,7], L. Callahan[4], S. M. Cha[11], K. Y. Chae[11], A. M. Clark[4], B. Frentz[4], M. R. Hall[4], A. Gula[4], S. Henderson[4], R. Kelmar[4], M. S. Kwag[11], I. Indelicato[1], M. La Commara[12], D. Lattuada[1,10], Q. Liu[4], J. Long[4], M. Mazzocco[13], A. Majumdar[4], S. McGuinness[4], A. Nelson[4], A. A. Oliva[1,2,3], P. O'Malley[4], P. M. Prajapati[1], G. G. Rapisarda[1], S. Romano[1,2,3], M. L. Sergi[1,2], C. Seymour[4], M. Skulski[4], C. Spitaleri[1,2], J. Wilkinson[4]

[1] Laboratori Nazionali del Sud-INFN, Catania, Italy
[2] Dipartimento di Fisica e Astronomia "Ettore Maiorana", Universitá di Catania, Catania, Italy
[3] Centro Siciliano di Fisica Nucleare e Struttura della Materia, Catania, Italy
[4] Department of Physics, University of Notre Dame, Notre Dame, IN, USA
[5] Nuclear Physics Institute of the Czech Academy of Sciences, 250 68 Řež, Czech Republic
[6] Universitá di Perugia, Perugia, Italy
[7] INFN Perugia, Perugia, Italy
[8] Technische Universität Darmstadt, Fachbereich Physik, Institut für Kernphysik, Darmstadt, Germany
[9] GSI Helmholtzzentrum für Schwerionenforschung GmbH, Theorie, Darmstadt, Germany
[10] Facoltá di Ingegneria e Architettura, Universitá degli Studi di Enna Kore, Enna, Italy
[11] SKKU Sungkyunkwan University, Seoul, Korea
[12] INFN and Universitá of Napoli, Napoli, Italy
[13] Dipartimento di Fisica e Astronomia, University of Padova and INFN-Sezione di Padova, Padova, Italy

Received: 20 April 2020 / Accepted: 29 July 2020

Communicated by Alexandre Obertelli

Abstract Nuclear reactions play a key role in the framework of the Big Bang Nucleosynthesis. A network of 12 principal reactions has been identified as the main path that drove the elemental nucleosynthesis in the first 20 min of the history of the Universe. Among them an important role is played by neutron-induced reactions, which, from an experimental point of view, are usually a difficult task to be measured directly. Nevertheless big efforts in the last decades have led to a better understanding of their role in the primordial nucleosynthesis network. In this work we apply the Trojan Horse Method to extract the cross section at astrophysical energies for the ^{3}He(n,p)^{3}H reaction after a detailed study of the ^{2}H(^{3}He,pt)H three-body process. Data extracted from the present measurement are compared with other published sets.

1 Introduction

One of the foundation stones of the Big Bang model, together with the Hubble expansion and the Cosmic Microwave Background (CMB) radiation [1], is the Big Bang Nucleosynthesis (BBN). BBN probes the Universe at very early times, the so called radiation dominated era, from a fraction of a second to a few minutes. It involves reactions that occur at temperatures below 1 MeV, and naturally plays a key role in forging the connection between cosmology and nuclear physics [2–4].

Focusing on the products of the BBN, according to the Standard Big Bang Nucleosynthesis model (SBBN), only the formation of light nuclei (^{2}H,^{3,4} He,^{7} Li) is predicted in observable quantities, starting from protons and neutrons. Great uncertainties affect observational ^{3}He abundance, as well as the attempt to estimate its primordial value, thus it is not reliable in the SBBN model validation. The remaining elemental abundances, both observed and calculated are consistent, with the exception of ^{7}Li [5]. A comparison between the primordial abundances deduced from WMAP and Planck CMB precise measurements and the calculated ones con-

[a] e-mail: rgpizzone@lns.infn.it (corresponding author)

Published online: 05 August 2020

Table 1 Nuclear reactions of greatest relevance for Big Bang nucleosynthesis, labelled from 1 to 12

(1) $n \leftrightarrow p$	(2) $p(n,\gamma)d$
(3) $d(p,\gamma)^3He$	(4) $d(d,p)t^{(*)}$
(5) $d(d,n)^3He^{(*)}$	(6) $^3He(n,p)t$
(7) $t(d,n)^4He$	(8) $^3He(d,p)^4He^{(*)}$
(9) $^3He(\alpha,\gamma)^7Be$	(10) $t(\alpha,\gamma)^7Li$
(11) $^7Be(n,p)^7Li$ and $^7Be(n,\alpha)^4He^{(*)}$	(12) $^7Li(p,\alpha)^4He^{(*)}$

The reactions already measured with the Trojan Horse method are marked with a [a] symbol. Reaction (6) will be studied in the present paper

strains the baryon-to-photon ratio, η, which is the only free parameter in the presently accepted model of the SBBN. A recent observation yields $\eta = 6.16 \pm 0.15 \times 10^{-10}$ [6], which is the value that is usually adopted.

BBN nucleosynthesis requires several nuclear physics inputs and, among them, the major role is played by the nuclear reaction rates. Due to the relatively small amount of key nuclear species involved in the BBN nuclear reaction network, only 12 reactions play a major role [7]. Some of those reactions involve neutrons and radioactive ions and are currently not known with sufficient precision (see Table 1). The reaction rates are calculated from the available low-energy reaction cross sections. They are also a fundamental input for a number of other still unsolved astrophysical problems, e.g. the so called "lithium destruction" either in the Sun or in other galactic stars [8,9]. Cross sections should be measured in the astrophysically relevant energy window [10], of the order of few hundreds of keV. In the last decades these reactions have been widely studied and, in particular, great efforts have been devoted to their study by means of direct measurements at the relevant astrophysical energies, sometimes in underground laboratories [11–13].

In particular, the ^{3}He(n,p)^{3}H reaction is one of the most relevant neutron induced processes in BBN and has a strong impact on the primordial ^{3}He and ^{7}Li production. At the temperatures relevant for predicting Big Bang yields, the reaction rate is determined by the ^{3}He(n,p)^{3}H cross section in the energy range $0 \leq E_{cm} \leq 0.4$ MeV. The first studies of this reaction were performed by Coon et al. [14] in 1950 in the $0.1 \leq E_{cm} \leq 30$ MeV using a neutron beam. Errors turned out to be around 30%. Other measurements, more focused at lower energies, were conducted by Batchelor et al. [15] (direct one, $0.1 \leq E_{cm} \leq 1$MeV), Gibbons et al. [16] (inverse measurement) and Costello et al. [17] who measured directly in the range $0.3 \leq E_{cm} \leq 1.1$ MeV. Theoretical predictions are also available, the most recent one carried out by Drosg et al. [18], which covered a wider energy range. Reaction rates were then calculated for astrophysical applications by Brune et al. [19], Adahchour et al. [20] and Smith et al. [21]. They all show a similar trend at temperatures of astrophysical interest while the reaction rate calculated by Caughlan and Fowler [22] is considerably higher. In the energy range of interest, the existing data are therefore sparse and mostly measured more than 50 years ago after facing tough experimental challenges, thus resulting several times in errors as high as 30% depending on the energy.

Alternative and complementary ways to obtain the bare nucleus cross section, σ, have been provided by indirect methods such as the Coulomb dissociation method [23,24] and the Asymptotic Normalization Coefficient (ANC) method [25,26]. Among those ones, the Trojan–Horse method (THM) [27] is particularly suited to investigate, at astrophysical energies, binary reaction induced by neutrons or charged particles by using appropriate three-body reactions. It allows one to avoid both Coulomb and centrifugal barrier suppression and electron screening effects, thus very low energies can be reached and extrapolations are not needed. Moreover, it may be used with neutron induced reactions, radioactive isotopes, as well as to determine cross sections of neutron induced reactions on unstable isotopes.

The THM in particular has shown its great power for measuring reaction rates for the BBN in the whole energy range of interest. This is reviewed in Ref. [28] and has been extended to reactions induced by unstable nuclei of interest for BBN as in Refs. [29,30]. The same methodology has been adopted for the ^{3}He(n,p)^{3}H reaction and will be reported in the present paper.

2 Trojan Horse Method: generalities

The THM, first suggested by Baur [31] and then defined in the present formulation [27], aims at obtaining the cross section of the binary process $x + A \rightarrow b + B$ at astrophysical energies by measuring the TH reaction, that is, the $2 \rightarrow 3$-particle process $a + A \rightarrow b + B + s$, in the quasi-free (QF) kinematic regime. Under these conditions, the Trojan Horse (TH) particle a, which has a dominant $s - x$ cluster structure, is propagating at energies above the Coulomb and centrifugal barrier and after penetration, undergoes breakup in the nuclear field of particle A. There, particle x interacts with target A while projectile s, also called the *spectator*, flies away practically without changing its momentum. From the measured three-body cross section, the energy dependence of the binary sub-process $x + A \rightarrow b + B$ is determined. The QF reaction used to extract this cross section is schematically depicted in Fig. 1. For the details on the theoretical formalism please refer to [32–36] and references therein. Since the projectile energy is chosen larger than the $A - a$ Coulomb barrier E_C^{aA}, the probability to find a within the nuclear field of A, which is given by the squared modulus of the scattering wave function describing

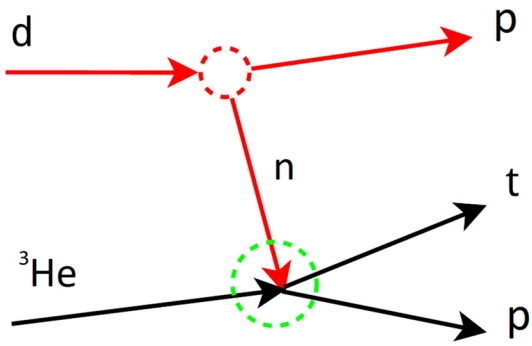

Fig. 1 Diagrams describing the TH reaction ^{2}H(^{3}He,pt)H in the QF kinematics, proceeding through the direct ^{3}He(n,p)^{3}H sub-reaction

their relative motion, is not suppressed leading to a finite probability that A can be in the proximity of x. This is an heuristic explanation of the possibility to explore the whole Gamow window by using the THM, with no need of extrapolation. A drawback of the present formulation of THM is that the absolute value of the cross section has to be determined by scaling the TH data to available direct measurements, at energies where electron screening is negligible.

It is important to note that the $a + A \rightarrow b + B + s$ reaction can proceed through different reaction mechanisms besides QF so that an investigation of the reaction mechanisms populating the $b + B + s$ final state is necessary before applying the THM formalism. In particular, the QF reaction process gives a dominant contribution to the cross section in a restricted region of the three-body phase space, where the relative momentum p_{xs} of the fragments s and x is close to zero (QF kinematical condition) or $\hbar/p_{xs}$ is small compared to the bound state $s - x$ wave number. Owing to quantum mechanics, this entails that the relative distance of x and s is very large and we can assume that s acts as a spectator to the $x - A$ interaction, the strong interaction being of short range.

The THM has been successfully applied to the measurement of bare-nucleus cross sections of reactions between charged particles at sub-Coulomb energies. Many validity tests were also performed for it like the pole invariance test which was positively satisfied, for details see [37,38]. The method has been used in the last three decades to explore nucleosynthesis reactions other than the primordial ones in different sites, e.g., massive stars [39], AGB stars [40–43], LiBeB depletion in stars [44–48] as well as novae [49–52] .

In recent years, neutron induced reactions [53–56] have been addressed as well, using deuterons as TH nuclei to transfer neutrons, while protons act as spectators. Following the simple plane-wave impulse approximation (PWIA), the three-body reaction cross section of the reaction of interest can be factorized into three terms as:

$$\frac{d^3\sigma(E)}{d\Omega_\alpha d\Omega_{^3He} dE_n} \propto KF \cdot |\phi(p_s)|^2 \cdot \left(\frac{d\sigma}{d\Omega}\right)^{HOES} \quad (1)$$

where

(i) KF is a kinematical factor containing the final-state phase-space factor, which is a function of the masses, momenta, and angles of the outgoing particles [35];
(ii) $|\phi(p_s)|^2$ is the modulus-squared Fourier transform of the radial wave function $\chi(r_{p_n})$ describing the $p - n$ inter-cluster motion, given by the Hulthén function.
(iii) $\left(\frac{d\sigma}{d\Omega}\right)^{HOES}$ is the half-off-energy-shell (HOES) differential cross section of the reaction of interest at the center-of-mass energy E_{cm}.

The theory of the TH for resonant and non resonant binary sub-reactions is presented in detail in Ref. [57]. As is sketched in Fig. 1, this work will present the investigation of the ^{2}H(^{3}He,pp)^{3}H quasi-free reaction, thus applying the THM in order to retrieve the cross section for the ^{3}He(n,p)^{3}H reaction at astrophysical energies.

3 Experimental setup

In the preparatory phase the best angular and energy regions were determined using a simulation to favour the QF reaction mechanism and to discriminate it as much as possible from other processes occurring in the target. In particular the QF angular pairs, i.e. angular couples for which the spectator momentum is nearly zero were calculated and detectors placed in order to cover this kinematic region [35]. The ^{3}He beam, delivered at a total kinetic energy of 9 MeV by the FN Tandem accelerator at the Nuclear Physics Laboratory of the University of Notre Dame, was impinged on a 100 μg/cm^2 isotopically enriched (up to 98%) deuterated polyethylene target, which was manufactured at the INFN-LNS target laboratory. Detectors were placed as sketched in Fig. 2. Three silicon position sensitive detectors (PSD 1–3), 1000 μm thick were used; PSD1 was coupled with a 35 μm thin, 10 $\times$ 50 mm^2 silicon detector for particle identification, while no particle identification was required for the other two detectors, thus optimizing the energy resolution of the apparatus. Two symmetrical monitor detectors were placed on both sides of the beam at 60° to check the beam symmetry. Another point-like silicon detector (PL1) was placed at 45° for on-line monitoring of the target thickness and its deuterium content during the experiment. A metal grid, with equally spaced slits, was placed in front of each PSD in order to perform an accurate angular calibration.

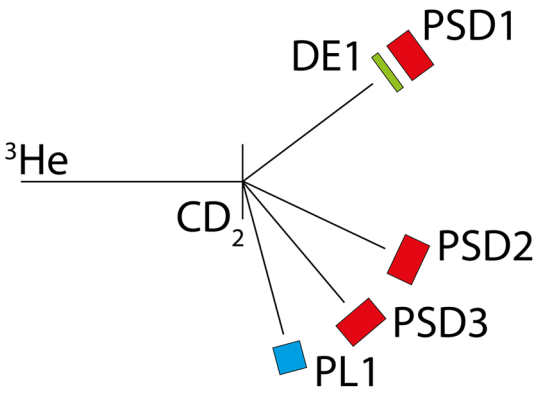

Fig. 2 Experimental setup employed for studying the TH reaction ^{2}H(^{3}He,pt)H in QF kinematics

Table 2 Angular position, distance and covered angular range from central position of the PSD1, PSD2, PSD3 and ΔE_1 detectors as sketched in Fig. 2 and as described in the text

Detector	Central angle (°)	Distance (cm)	$\Delta\theta$ (°)
PSD1	10.0	35	± 4
PSD2	15.0	20	± 7
PSD3	25.0	35	± 4
ΔE_1	10.0	33	± 4.3

As a first stage of the measurements, devoted calibration runs were performed for energy and angular calibration. Thanks to the spatial resolution of PSD and to the accurate positioning of the detectors which were measured by optical means, an angular resolution of about 0.15 was calculated. This is required by THM for an improved spectator momentum resolution which is crucial for QF mechanism selection. The energy resolution of PSD detectors was tested prior the experiment and turned out to be around 0.8%. This leads, thanks to the so-called Magnifying glass effect [53] to an overall relative energy resolution of about 25 keV.

Angular positions of the PSD's detectors and geometrical features of the experimental set-up are summarized in Table 2. Calibration runs were performed using ^{241}Am and ^{148}Gd alpha sources and proton and alpha scattering on a gold target at various energies ranging from 3.5 to 9 MeV. The trigger for the data acquisition was made via the logic coincidence of PSD1 with any of the three PSD's placed on the opposite side with respect the beam axis. Then data were stored in the DAQ system provided by the University of Notre Dame and converted to ROOT format for offline analysis.

4 Data analysis

The first point of the data analysis is the identification of the three-body process of interest among those occurring in the target, which leads to the detection in coincidence of a proton and a triton in two out of the three detectors. For this purpose, a particle identification is performed for PSD1 via the ΔE/E technique as reported in Fig. 3. Many loci are populated and in particular those related to deuterons and tritons are present, the latter being selected by means of the graphical cut. For further analysis only events corresponding to the tritium locus in ΔE/E matrices are used. In particular the scattered beam-spot is evident in the ^{3} He locus. The recoil ^{2} H spot is also evident in the deuteron locus at an energy of about 6.7 MeV in Fig. 3.

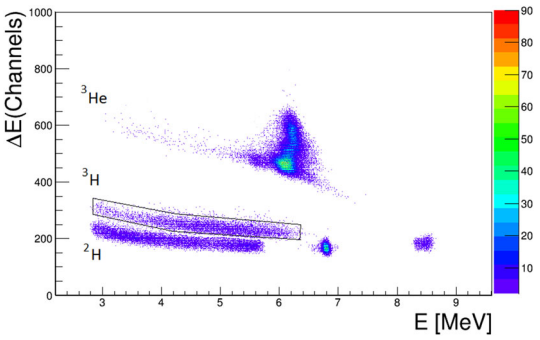

Fig. 3 ΔE/E plot for PSD1 for a typical run of the ^{2}H(^{3}He,pt)H reaction. The black selection represents events identified as tritons

Energies and position signals for particles in coincidence are then calibrated appropriately as discussed above. In the present paper only the coincidence between PSD1 and PSD2 was analyzed. The other coincidence, between detectors PSD1 and PSD3, which explores higher energies in the E_{cm} range, will be investigated in the future. In the scatter-plot reported in Fig. 4 the kinematic locus of the detected t and p coincidences (red points) is compared with a kinematic simulation for the same conditions and for angles ranging from $9° \leq \theta_t \leq 11°$ and $10° \leq \theta_p \leq 12°$ (black dots). A clear agreement is evident in the whole explored energy range.

Once the angle and energy of the two detected particles are obtained, the energy and the angle of the third, undetected, particle is reconstructed from energy and momentum conservation. This allows to extract the Q-value of the three-body reaction as shown in Fig. 5. A Gaussian fit is drawn as a red line and gives an average value of -1.55 ± 0.14 MeV which should be compared with an expected value of $Q = -1.46$ MeV [58]. The agreement between expected and measured values in Figs. 4 and 5 validates the energy calibration. Henceforth only events with $-1.7 \leq Q \leq -1.4$ MeV will be considered for further analysis, thus leading to a clear identification of the ^{2}H(^{3}He,pt)H process.

4.1 Identification of the quasi-free break-up

When the selection of the three-body process is well established the next step in the data analysis is the identifica-

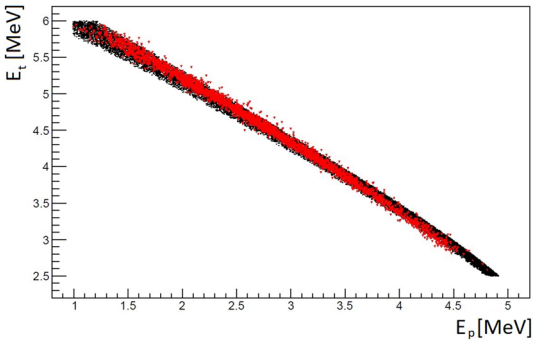

Fig. 4 Kinematic locus for tritons detected in PSD1 and protons from PSD2 for $9° \leq \theta_t \leq 11°$ and $10° \leq \theta_p \leq 12°$. The experimental data (red circles) are compared with a kinematical simulation (black dots) for the ^{2}H(^{3}He,pt)H reaction

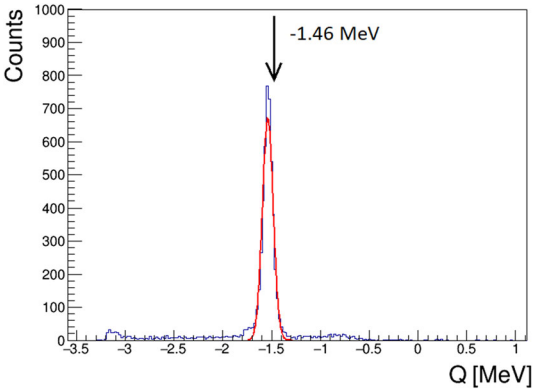

Fig. 5 Q-value spectrum for PSD1-PSD2 coincidences after tritons are selected in PSD1. A Gaussian fit is superimposed as a red line. The calculated value of − 1.46 MeV is in fair agreement and is indicated by the black arrow

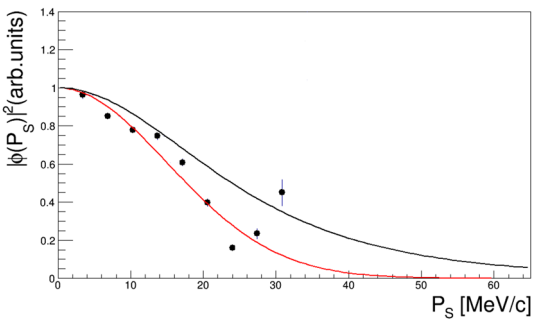

Fig. 6 Momentum distribution in arbitrary units for the proton inside the TH deuteron. A Gaussian fit is depicted (red line) together with the theoretical momentum distribution given by the Hulthén function (black solid line)

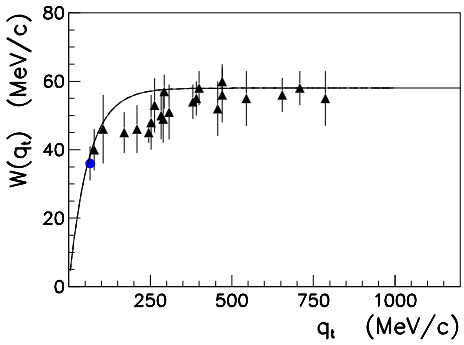

Fig. 7 Momentum distribution width as a function of the transferred momentum q_t. The blue circle marks data corresponding to the present measurement while black symbols as well as the solid line are taken from [61] and references therein

tion of the QF mechanism and consequently its separation from other processes. After studying the relative energy as it is shown in Ref. [47] we can exclude the presence of any sequential mechanism leading to 2p and ^{3}H particles in the final state. Hence, to verify whether the quasi-free process is taking place or not, the extraction of the momentum distribution of the spectator proton inside the TH nucleus (deuteron) has to be extracted and carefully analyzed.

The momentum distribution is extracted following the prescriptions of [60]; inverting Eq. (1) in terms of the momentum distribution leads to

$$|\phi(p_s)|^2 \propto \frac{d^3\sigma(E)}{d\Omega_\alpha d\Omega_{^7Li} dE_\alpha} / KF \cdot \left(\frac{d\sigma}{d\Omega}\right)^{HOES} \quad (2)$$

Assuming a narrow energy range ($\Delta E_{cm} = 200$ keV in the present case) the binary HOES cross section is nearly constant and therefore a division of the triple differential cross section by the KF gives the momentum distribution $|\phi(p_s)|^2$ in arbitrary units. This quantity is plotted in Fig. 6. A Gaussian fit is superimposed in red color (FWHM $= 35 \pm 5$ MeV/c) while the black line represents the theoretical Hulthén function as discussed in Ref. [59]. It is clearly evident that the present momentum distribution is distorted and narrowed, an effect already pointed out for deuteron and other nuclides in Ref. [61]. In fact, in this case, a transferred momentum $q_t = 80$ MeV/c is calculated and the corresponding momentum distribution width fits pretty well with what is reported in the literature for deuteron acting as Trojan horse nuclei [61]. This is evident from Fig. 7 where the blue circle represents the present data. Other data from the literature as well as a fit to them with an empirical function discussed in Ref. [61] are depicted there.

This observation is a clear signature, taking into account its distortions as recommended in Refs. [61,62], of the QF break-up since the momentum distribution of the spectator particle is the variable which is most sensitive to the nature of the mechanism. For further analysis only events with $p_s \leq 25$ MeV/c were taken into account, being the bulk of the QF contribution in the ^{2}H(^{3}He,pt)H process.

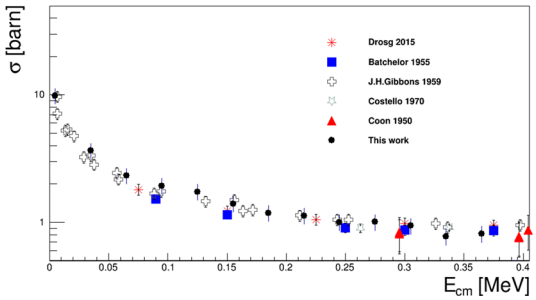

Fig. 8 Binary cross section (black circles) after including the penetration factor and normalized to direct data from [15,16,18] for the ^{3}He(n,p)^{3}H sub-reaction extracted via the TH reaction ^{2}H(^{3}He,pt)H in QF kinematics, as discussed in the text. Only errors from statistics and normalization are shown

5 Results and concluding remarks

After the selection of events related to the quasi-free breakup, as discussed above, standard THM prescriptions are followed. Using the post-collision approach for the definition of $E_{cm} = E_{12} - Q_{2b}$ (where Q_{2b} is the two body reaction Q-value), the triple differential cross section, is divided by the product $KF \cdot |\phi(p_s)|^2$ according to Eq. (1). As shown in Ref. [62] the distorted momentum distribution, which has been measured experimentally in this present case, is used. The result yields the HOES binary cross section of the ^{3}He(n,p)^{3}H reaction in arbitrary units. The THM data must be multiplied for the penetration factor in order to be compared and normalized to direct data (see for example Refs. [53,54]). In the case of a neutral particle at low energies and with l=0 the cross section energy trend may be approximated by the $1/v$ velocity-factor which should be multiplied with the TH data. The results after applying this correction are shown in Fig. 8. The cross section was normalized to the direct data from [15,16,18] in the energy range $0.2 \leq E_{cm} \leq 0.35$ MeV. A remarkable agreement shows up in the whole energy range. Statistical errors as well as normalization errors were fully taken into account yielding an average 10% relative error for the cross section extracted via THM. As far as the error on the quantities contributing to E_{cm}, we apply the error propagation law assuming an uncertainty on E_p and E_t of 0.8% and an error on the position $\Delta\theta_p \approx \Delta\theta_t \approx 0.15^o$.

In conclusion, the cross section of the ^{3}He(n,p)^{3}H reaction, was measured in the energy range important for Big Bang nucleosynthesis using the THM. Once more the method has proved to be important for measuring neutron induced reactions of astrophysical interest at thermal energies. The present data set confirms, within the experimental errors, a very satisfying agreement of the measured data with direct and inverse reaction data from the literature [15,16] in the energy region $0.03 \leq E_{cm} \leq 0.3$ MeV. We also remark that the present data are the only ones (together with [16]) available below 0.1 MeV. Further analysis is necessary in order to extend the measurement to higher energies, using data from the PSD1-PSD3 coincidence. This will allow to calculate the reaction rate in an extended energy interval and to evaluate the astrophysical impact of the present measurement. Nevertheless the present data sets is coherent with previous determinations thus suggesting minor changes for the calculated primordial abundances with respect to the reaction rates currently adopted for BBN models.

Acknowledgements We thank the staff of the LNS target laboratory, for target preparation as well as the Nuclear Science Laboratory (supported by Grant the National Science Foundation under grant number NSF PHY-1713857) staff at the University of Notre Dame for their invaluable efforts. J.M, G.D. and V. B. were supported by MEYS Czech Republic under the project EF16-013/0001679. The authors acknowledge "Finanziamenti di linea 2" and "Starting Grant 2020" by University of Catania. This work was also supported in part by the National Research Foundation of Korea (NRF) Grant funded by the Korea government (MSIT) (Nos. 2020R1A2C1005981 and 2016R1A5A1013277).

Data Availability Statement This manuscript has no associated data or the data will not be deposited. [Authors' comment: Data are stored in INFN LNS computer disks and are available to the community upon request].

References

1. G. Steigman, Ann. Rev. Nucl. Part. Sci. **57**, 463 (2007)
2. B.D. Fields, S. Sarkar, J. Phys. **G33**, 220 (2006)
3. A. Coc, S. Goriely, Y. Xu, M. Saimpert, E. Vangioni, Astrophys. J. **744**, 18 (2012)
4. R.H. Cyburt, B.D. Fields, K.A. Olive, T.H. Yeh, Rev. Mod. Phys. **88**, 015004 (2016)
5. G. Israelian, Nature **489**, 37 (2012)
6. E. Komatsu et al., Astrophys. J. Suppl. **192**, 18 (2011)
7. E.W. Kolb, M.S. Turner, *The Early Universe* (Addison-Wesley, Boston, 1990)
8. R. Weymann, E. Moore, Astrophys. J. **137**, 552 (1963)
9. D. Ezer, A.G.W. Cameron, Icarus **1**, 422 (1963)
10. C. Iliadis, *Nuclear Physics of Stars* (Wiley, Hoboken, 2007)
11. C. Rolfs, Prog. Part. Nucl. Phys. **46**, 23 (2001)
12. R. Bonetti et al., Phys. Rev. Lett. **82**, 5205 (1999)
13. C. Casella et al., Nucl. Phys. A **706**, 203 (2002)
14. J.H. Coon, Phys. Rev. **80**, 488 (1950)
15. R. Batchelor, R. Aves, T.H.R. Skyrme, Rev. Sci. lnstr. **26**, 1037 (1955)
16. J.H. Gibbons, R.L. Macklin, Phys. Rev. **114**, 571 (1959)
17. D.G. Costello, S.J. Friesenhahn, W.M. Lopez, Nucl. Sci. Eng. **39**, 409 (1970)
18. M. Drosg , N. Otuka, INDC (AUS)-0019 (2015)
19. C.R. Brune, K.I. Hahn, R.W. Kavanagh, P.R. Wrean, Phys. Rev. **C60**, 015801 (1999)
20. A. Adahchour, P. Descouvemont, J. Phys. G Nucl. Part. Phys. **29**, 395 (2003)
21. M.S. Smith, L.H. Kawano, R.A. Malaney, Astrophys. J. Suppl. Ser. **85**, 219 (1993)
22. G.R. Caughlan, W.A. Fowler, At. Data Nucl. Data Tables **40**, 283 (1988)
23. G. Baur, C.A. Bertulani, H. Rebel, Nucl. Phys. A **458**, 188 (1986)
24. C.A. Bertulani, A. Gade, Phys. Rep. **485**, 195 (2010)

25. A. Mukhamezhanov et al., Phys. Rev. C **78**, 0158042008 (2008)
26. G.G. Kiss et al., Phys. Lett. B. **807**, 135606 (2020)
27. C. Spitaleri, in *Problems of Fundamental Modern Physics, II* : Proceedings, Ed. by R. Cherubini,P. Dalpiaz, and B. Minetti (World Sci., 1991), p. 21 (1991)
28. R.G. Pizzone, R. Spartá, C. Bertulani et al., Astrophys. J. **786**, 112 (2014)
29. L. Lamia et al., Astrophys. J. **850**, 175 (2017)
30. L. Lamia, M. Mazzocco, R.G. Pizzone et al., Astrophys. J. **879**, 23 (2019)
31. G. Baur, C.A. Bertulani, H. Rebel, Nucl. Phys. A **458**, 188 (1986)
32. S. Typel, H.H. Wolter, Few-Body Syst. **29**, 75 (2000)
33. S. Typel, G. Baur, Ann. Phys. (N.Y.) **305**, 228 (2003)
34. C. Spitaleri et al., Nucl. Phys. A **719**, 99c (2003)
35. C. Spitaleri, M. La Cognata, L. Lamia, A.M. Mukhamedzhanov, R.G. Pizzone, Eur. Phys. J. A **52**, 77 (2016)
36. C. Spitaleri, M. La Cognata, L. Lamia, R.G. Pizzone, A. Tumino, Eur. Phys. J. A **55**, 161 (2019)
37. R.G. Pizzone, L. Lamia, C. Spitaleri et al., Phys. Rev. C **83**, 045801 (2011)
38. R.G. Pizzone, C. Spitaleri, C. Bertulani et al., Phys. Rev. C **87**, 025805 (2013)
39. A. Tumino, C. Spitaleri, M. La Cognata et al., Nature **557**, 687–690 (2018)
40. S. Palmerini, M.L. Sergi, M. La Cognata, L. Lamia et al., Astrophys. J. **764**, 128 (2013)
41. R.G. Pizzone, G. D'Agata, C. Spitaleri et al., Astrophys. J. **836**, 57 (2017)
42. I. Indelicato, M. La Cognata et al., Astrophys. J. **845**, 19 (2017)
43. G. D'Agata, R.G. Pizzone et al., Astrophys. J. **860**, 61 (2018)
44. G.G. Rapisarda et al., Eur. Phys. J **A54**, 189 (2018)
45. A. Cvetinovic et al., Phys. Rev. C **97**, 065801 (2018)
46. M. Aliotta, C. Spitaleri et al., Eur. Phys. J. A **9**, 435 (2000)
47. L. Lamia et al., Nuovo Cimento C **31**, 423–431 (2008)
48. L. Lamia, C. Spitaleri, E. Tognelli et al., Astrophys. J. **811**, 99 (2015)
49. M.L. Sergi, C. Spitaleri, M. La Cognata et al., Phys. Rev. C **91**, 065803 (2015)
50. S. Cherubini et al., Phys. Rev. C **92**, 015805 (2015)
51. R.G. Pizzone, B. Roeder, M. Mckluskey et al., Eur. Phys. J. A **52**, 24 (2016)
52. M. La Cognata, R.G. Pizzone et al., Astrophys. J. **846**, 65 (2017)
53. M. Gulino et al., J. Phys. **37**, 125105 (2010)
54. M. Gulino et al., Phys. Rec. **C87**, 012801 (2013)
55. G.L., Guardo, C. Spitaleri, L. Lamia, et al., Phys. Rev. C **95**, 025807 (2017)
56. G.L. Guardo, C. Spitaleri, L. Lamia et al., Eur. Phys. J. A **55**, 211 (2019)
57. R.E. Tribble et al., Rep. Prog. Phys. **77**, 10690 (2014)
58. Qtool: https://t2.lanl.gov/nis/data/qtool.html
59. L. Lamia et al., Phys. Rev. C **85**, 025805 (2012)
60. S. Barbarino, M. Lattuada, F. Riggi, C. Spitaleri, D. Vinciguerra, Phys. Rev. C **21**, 1104 (1980)
61. R.G. Pizzone et al., Phys. Rev. C **80**, 025807 (2009)
62. R.G. Pizzone, C. Spitaleri, S. Cherubini et al., Phys. Rev. C **71**, 058801 (2005)